

Supplementary Material

Constructing interconnected spherical hollow conductive networks in silver platelets/reduced graphene oxide foam/epoxy nanocomposites for superior electromagnetic interference shielding effectiveness

Chaobo Liang^a, Ping Song^a, Hua Qiu^{a,e}, Yali Zhang^a, Xiangteng Ma^b, Fengqi Qi^a, Hongbo Gu^c, Jie Kong^a, Dapeng Cao^d, Junwei Gu^{a*}

^aMOE Key Laboratory of Material Physics and Chemistry under Extraordinary Conditions, Shaanxi Key Laboratory of Macromolecular Science and Technology, Department of Applied Chemistry, School of Science, Northwestern Polytechnical University, Xi'an, Shaanxi, 710072, P.R. China.

^bSchool of Mechanics, Civil Engineering and Architecture, Northwestern Polytechnical University, Xi'an, Shaanxi, 710072, P.R. China.

^cShanghai Key Lab of Chemical Assessment and Sustainability, School of Chemical Science and Engineering, Tongji University, Shanghai, 200092, P.R. China.

^dState Key Lab of Organic-Inorganic Composites, Beijing University of Chemical Technology, Beijing, 100029, P.R. China.

^eSchool of Materials Science and Engineering, Henan University of Science and Technology, Luoyang, 471023, P. R. China.

Corresponding Authors: gjw@nwpu.edu.cn or nwpugjw@163.com (J. Gu)

S1 Experimental Section

S1.1 Materials

Bisphenol F epoxy of Epon 862 and curing agent of EK3402 were both purchased from Hexion Inc (America), and the corresponding chemical structures are shown in Fig. S1. Silver platelets (AgPs, $\geq 99.9\%$, with diameter of $2\sim 3$ um and super diameter/thickness ratio of $25\sim 30$), were received from Shanghai Maoguo Nano Technology Co., Ltd. (Shanghai, China). Graphite flake (325 mesh, 99.8%) was provided by Alfa Aesar Co. Ltd. (China). Potassium persulfate ($K_2S_2O_8$, $\geq 99\%$), phosphorus pentoxide (P_2O_5 , $\geq 98\%$), potassium permanganate ($KMnO_4$, $\geq 99\%$), sulfuric acid (H_2SO_4 , 98%), hydrochloric acid (HCl , 37 wt%) and hydrogen peroxide (H_2O_2 , 30 wt%) were all purchased from Beijing Chemical Factory (Beijing, China). Dodecyl benzene sulfonate acid (DBSA, Mw of 326.49, 90% hydrolyzed) was supplied by Aladdin Reagent Co., Ltd. (Shanghai, China).

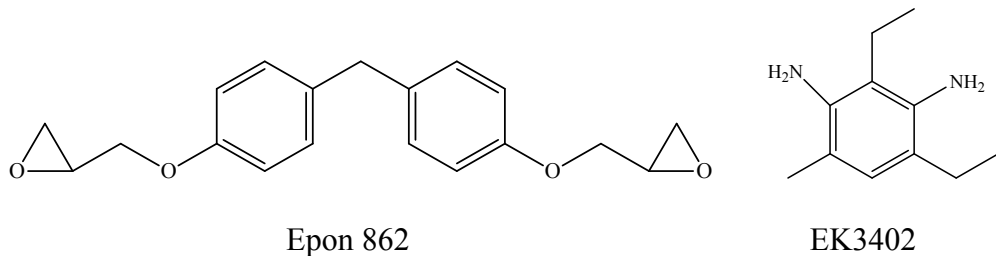


Fig. S1 Chemical structures of Epon 862 and EK3402.

S1.2 Characterizations

X-ray photoelectron spectroscopy (XPS) analyses of the samples were carried out using PHI5400 equipment (PE Corp., England). X-ray diffraction (XRD) crystallography was obtained on a Phillips PW3040-MPD diffractometer. Scanning electron microscope (SEM) morphologies of the samples were analyzed by VEGA3-LMH equipment (TESCAN Corp., Czech Republic). Atomic force microscope (AFM) morphologies of the samples were analyzed by Dimension FastScan and Dimension

Icon equipment (Bruker Corp., Germany). The size distribution of silver platelets in aqueous solution was measured by Winner 2000 laser particle size analyzer (Jinan Micro-Nano particle Instrument Co., Ltd., China). Electrical conductivities of the samples were measured using a RTS-8 Four Probe instrument (Guangzhou Four Probe Technology Corp., China). Characteristic EMI shielding parameters of the samples were tested by MS4644A Vector Network Analyzer instrument (Anritsu Corp., Japan) using wave-guide method at X-band according to ASTM D5568-08, and the corresponding dimension of the samples with length of 22.86 mm, width of 10.16 mm, and thickness of 3.00 mm.

S2 XPS spectra of the AgPs/GF and element contents for AgPs/GF and AgPs/rGF

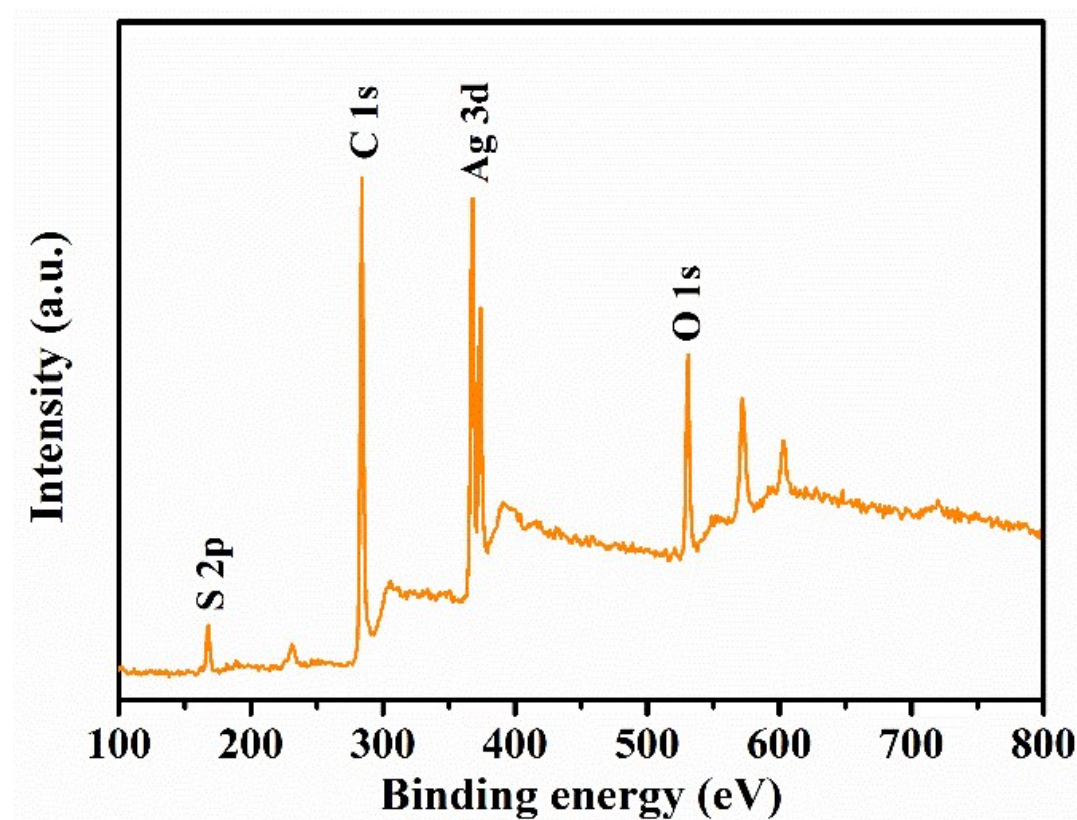


Fig. S2 XPS spectra of the AgPs/GF

Table S1. Element contents for AgPs/GF and AgPs/rGF

| Samples | Element content / % | | | |
|----------|---------------------|------|-----|-----|
| | C | O | Ag | S |
| AgPs/GF | 77.6 | 12.8 | 5.2 | 4.4 |
| AgPs/rGF | 89.1 | 9.2 | 1.7 | 0 |

S3 Mechanical properties of the AgPs/rGF

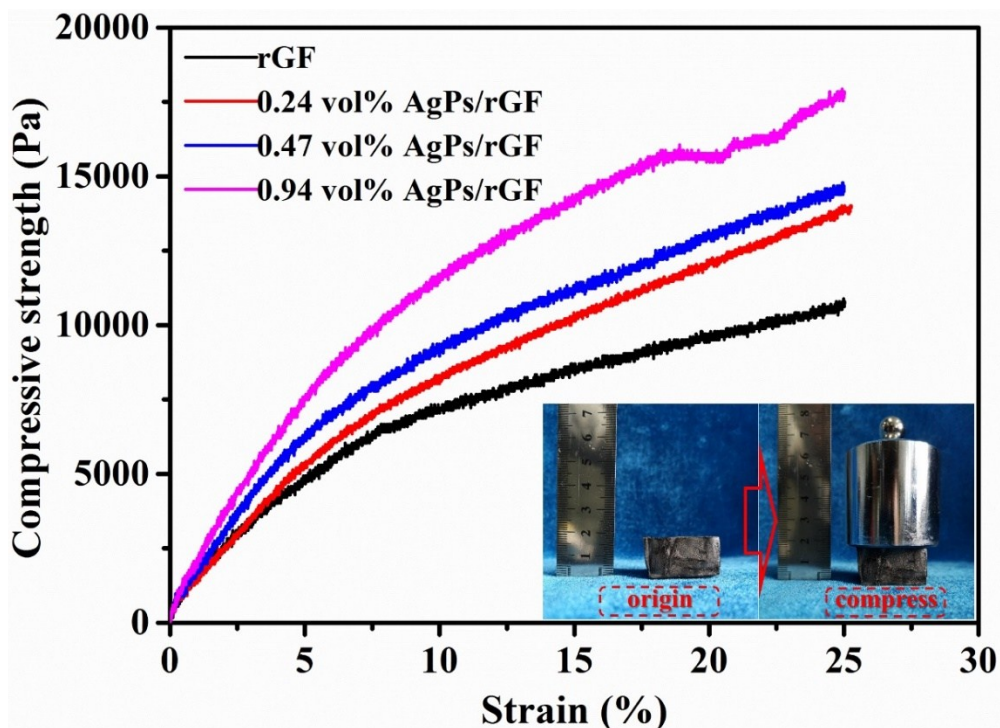


Fig. S3 Compressive stress-strain curves of the AgPs/rGF, in which AgPs/rGF with 0.94 vol% AgPs jacked up 500 g weight without significant collapse.

S4 Comparison of EMI SE_T for epoxy composites with other works

Table S2. Comparison of EMI SE_T for epoxy composites with other works

| Samples | Thickness | EMI SE _T | Frequency | Refs |
|-------------|-----------|---------------------|-----------|------|
| | (mm) | (dB) | (GHz) | |
| Graphene/EP | -- | 21 | 8.2~12.4 | 1 |

| | | | | |
|---|------|--------|----------|----|
| TAGA/EP | 4 | 27, 32 | 8~12 | 2 |
| GA/EP | 3 | 30 | 15~20 | 3 |
| Aligned rGO/EP | >0.1 | 38 | 0.4~4 | 4 |
| NCCFs/EP | 2 | 32 | 8.2~12.4 | 5 |
| NiCFs/EP | 5 | 32 | 8.2~12.4 | 6 |
| rGO/Fe ₃ O ₄ /EP | 2 | 37 | 8.2~12.4 | 7 |
| Ti ₃ SiC ₂ /Cu/EP | 1.8 | 27 | 9.6~12.4 | 8 |
| F-MWCNT/EP | 2.5 | 20.5 | 12~18 | 9 |
| Fe ₃ O ₄ /GA/EP | 3 | 35 | 8.2~12.4 | 10 |
| MWCNT@Ag/EP | 2 | 35 | 8.2~12.4 | 11 |
| SWNTs/EP | 3 | 38 | 8.2~12.4 | 12 |
| CNTs/rGF/EP | 3 | 36 | 8.2~12.4 | 13 |
| CNT _f /EP | 2 | 33 | 8.2~12.4 | 14 |
| MCF/EP | 2 | 46 | 8.2~12.4 | 15 |
| Ti ₃ C ₂ T _x /EP | 2 | 41 | 8.2~12.4 | 16 |
| PANI/MWCNT/TAGA/E P | 3 | 42 | 8.2~12.4 | 17 |
| CTBN-fMWCNTs/EP | 2 | 23 | 8.2~12.4 | 18 |
| Carbon/EP | 2 | 28 | 8~12 | 19 |
| RGO/Fe ₃ O ₄ /EP | 2 | 14 | 8.2~12.4 | 20 |
| GNPs/rGO/EP | 3 | 51 | 8.2~12.4 | 21 |
| NCCFs/EP | 2 | 41 | 8.2~12.4 | 22 |

Herein, EP, TGA, TAGA, GA, rGO, NCCFs, NiCFs, SWNTs, MCF, PANI, CTBN, GNPs and fMWCNT indicates epoxy, thermal graphene aerogels, thermally annealed anisotropic graphene aerogels, graphene aerogels, reduced graphene oxide, nickel coated carbon fibers, nickel-plated carbon fibers, single-walled carbon nanotubes, MXene/C hybrid foams, polyaniline, carboxy-terminated butadiene-acrylonitrile copolymer, graphene nanoplatelets, and functionalized multi-wall carbon nanotubes, respectively.

S5 Electromagnetic shielding effectiveness: theory and measurement

In a vector network analyzer, S_{11} , S_{12} , S_{21} and S_{22} represents reflection coefficient, transmission coefficient, back ward transmission coefficient and reverse reflection coefficient, respectively.

SE_T is evaluated from the S parameters using the following equations.²³

$$R = S_{11}^2 \quad (\text{Equation S1})$$

$$T = S_{12}^2 = S_{21}^2 \quad (\text{Equation S2})$$

$$A = 1 - T - R \quad (\text{Equation S3})$$

$$SE_T (\text{dB}) = -10 \log(S_{12}^2) = -10 \log(S_{21}^2) = -10 \log(T) \quad (\text{Equation S4})$$

$$SE_R (\text{dB}) = -10 \log(1 - S_{11}^2) = -10 \log(1 - R) \quad (\text{Equation S5})$$

$$SE_A (\text{dB}) = -10 \log\left(\frac{S_{12}^2}{1 - S_{11}^2}\right) = -10 \log\left(\frac{T}{1 - R}\right) \quad (\text{Equation S6})$$

EMI SE value depends on the dielectric and magnetic properties. Equation S7 is developed to quantify the contribution of SE_R and SE_A , to the overall EMI SE as a function of magnetic permeability.

$$SE_A (\text{dB}) = 20 \frac{d}{\delta} \log e = 20d \sqrt{\frac{\mu_r \omega \sigma_s}{2}} \log e \quad (\text{Equation S7})$$

Where, d is the thickness of materials, μ_r is the relative magnetic permeability, δ is the skin depth, σ_s is the frequency dependent conductivity, ω is the angular frequency, and ϵ_0 is the permittivity of the free space.

S6 Numerical simulation of the electromagnetic radiation process

S6.1 Definition of material properties

Table S3. Parameters of tissues

| Organs | ρ (kg/m ³) | c (J/kg K) | σ (S/m) | ϵ_r | ω (1/s) |
|-------------------------|-----------------------------|--------------|----------------|--------------|-----------------------|
| Skin | 1125 | 3437 | 2.16 | 41.79 | 2.00×10^{-2} |
| Bone | 1038 | 1300 | 2.10 | 44.80 | 4.36×10^{-4} |
| Inside the brain | 916 | 2300 | 0.13 | 5.51 | 4.58×10^{-4} |

Herein, ρ , c , σ , ϵ_r and ω represents the density, specific heat capacity, electric conductivity, dielectric constant and perfusion rate, respectively.

Table S4. Parameters of the AgPs/rGF/EP nanocomposites with 0.94 vol% AgPs.

| Parameters | 8 GHz | 10 GHz | 12 GHz |
|---|-------|--------|--------|
| Real part of the permittivity | 51.3 | 52.5 | 40.5 |
| Imaginary part of the permittivity | 34.7 | 39.2 | 33.4 |
| Electrical conductivity (S/m) | 45.3 | 45.4 | 45.7 |
| SE_A (dB) | 47.8 | 49.0 | 51.8 |
| SE_R (dB) | 6.0 | 5.9 | 5.8 |
| SE_T (dB) | 53.8 | 54.9 | 57.6 |

S6.2 Governing equations

COMSOL Multiphysics software is used to compute the numerical solutions of coupled electromagnetic equation. Maxwell's equations are used to solve the electromagnetic field distribution in the microwave cavity. The governing equation of the electric field wave is as follows:²⁴

$$\nabla \times \mu_r^{-1} (\nabla \times E) - k_0^2 \left(\epsilon_r - \frac{j\sigma}{\omega \epsilon_0} \right) E = 0 \quad (\text{Equation S8})$$

Where, μ_r , E , ϵ_r , σ , ω , ϵ_0 , j and k_0 represents the permeability of the material, electric field intensity, relative permittivity, electrical conductivity, angular frequency, free space permittivity, imaginary number i and wave number in free space, respectively.

Where, k_0 is defined as Equation S9:

$$k_0 = \omega \sqrt{\epsilon_0 \mu_0} = \frac{\omega}{c_0} \quad (\text{Equation S9})$$

Where, c_0 represents the speed of light in vacuum. And in 2D the electric field changes with the out-of-plane wave number k_z as:

$$E(x, y, z) = E_0(x, y) \exp(-ik_z z) \quad (\text{Equation S10})$$

Therefore, the wave equation is rewritten as Equation S11:

$$(\nabla - ik_z z) \times [\mu_r^{-1} (\nabla - ik_z z) \times E] - k_0^2 \epsilon_r E = 0 \quad (\text{Equation S11})$$

Where, z is the unit vector in the out-of-plane z direction.

References

1. J. J. Liang, Y. Wang, Y. Huang, Y. F. Ma, Z. F. Liu, J. M. Cai, C. D. Zhang, H. J. Gao and Y. S. Chen, *Carbon* 2009, **47**, 922-925.
2. X.-H. Li, X. Li, K.-N. Liao, P. Min, T. Liu, A. Dasari and Z.-Z. Yu, *ACS Appl. Mater. Interfaces*, 2016, **8**, 33230-33239.
3. Y. J. Wan, S. H. Yu, W. H. Yang, P. L. Zhu, R. Sun, C. P. Wong and W. H. Liao, *RSC Adv.*, 2016, **6**, 56589-56598.
4. N. Yousefi, X. Sun, X. Lin, X. Shen, J. Jia, B. Zhang, B. Tang, M. Chan and J. K. Kim, *Adv. Mater.*, 2014, **26**, 5480-5487.
5. J. M. Yang, Y. Q. Yang, H. J. Duan, G. Z. Zhao and Y. Q. Liu, *J. Mater. Sci-Mater. El.*, 2017, **28**, 5925-5930.

6. J. K. Pan, Y. Xu and J. J. Bao, *J. Appl. Polym. Sci.*, 2018, **135**, 1-10.
7. H. J. Liu, C. Z. Liang, J. J. Chen, Y. W. Huang, F. Cheng, F. B. Wen, B. B. Xu and B. Wang, *Compos. Sci. Technol.*, 2019, **169**, 103-109.
8. Y. Liu, X. Y. Jian, X. L. Su, F. Luo, J. Xu, J. B. Wang, X. H. He and Y. H. Qu, *J. Alloys Compd.*, 2018, **740**, 68-76.
9. J. T. Li, G. C. Zhang, H. M. Zhang, X. Fan, L. S. Zhou, Z. Y. Shang and X. T. Shi, *Appl. Surf. Sci.*, 2018, **428**, 7-16.
10. Y. M. Huangfu, C. B. Liang, Y. X. Han, H. Qiu, P. Song, L. Wang, J. Kong and J. W. Gu, *Compos. Sci. Technol.*, 2019, **169**, 70-75.
11. L. Wang, H. Qiu, C. B. Liang, P. Song, Y. X. Han, Y. X. Han, J. W. Gu, J. Kong, D. Pan and Z. H. Guo, *Carbon*, 2019, **141**, 506-514.
12. P. Song, C. B. Liang, L. Wang, H. Qiu, H. B. Gu, J. Kong and J. W. Gu, *Compos. Sci. Technol.*, 2019, **181**, 107698.
13. C. B. Liang, P. Song, A. J. Ma, X. T. Shi, H. B. Gu, L. Wang, H. Qiu, J. Kong, J. W. Gu, *Compos. Sci. Technol.*, 2019, **181**, 107683.
14. H. Mei, S. X. Zhou, P. Chang, Z. Y. Kong, Y. Zhao, C. Chen and L. F. Cheng, *Scripta Mater.*, 2019, **170**, 85-89.
15. L. Wang, H. Qiu, P. Song, Y. L. Zhang, Y. J. Lu, C. B. Liang, J. Kong, L. X. Chen and J. W. Gu, *Compos. Part A-Appl. S.*, 2019, **123**, 293-300.
16. L. Wang, L. X. Chen, P. Song, C. B. Liang, Y. J. Lu, H. Qiu, Y. L. Zhang, J. Kong and J. W. Gu, *Compos. Part B-Eng.*, 2019, **171**, 111-118.
17. Y. M. Huangfu, K. P. Ruan, H. Qiu, Y. J. Lu, C. B. Liang, J. Kong and J. W. Gu, *Part A-Appl. S.*, 2019, **121**, 265-272.
18. X. Fan, G. C. Zhang, J. T. Li, Z. Y. Shang, H. M. Zhang, Q. Gao, J. B. Qin, X. T. Shi, *Part A-Appl. S.*, 2019, **121**, 64-73.

19. Z. M. Shen and J. C. Feng, ACS Sustainable Chem. Eng., 2019, **7**, 6259-6266.
20. Y. C. Liu, M. P. Lu, K. Wu, S. Yao, X. X. Du, G. K. Chen, Q. Zhang, L. Y. Liang and M. G. Lu, Compos. Sci. Technol., 2019, **174**, 1-10.
21. C. B. Liang, H. Qiu, Y. Y. Han, H. B. Gu, P. Song, L. Wang, J. Kong, D. P. Cao and J. W. Gu, J. Mater. Chem. C, 2019, **7**, 2725-2733.
22. H. J. Duan, H. X. Zhu, J. M. Yang, J. F. Gao, Y. Q. Yang, L. Xu, G. Z. Zhao, Y. Q. Liu, Part A-Appl. S., 2019, **118**, 41-48.
23. L. C. Jia, G. Q. Zhang, L. Xu, W. J. Sun, G. J. Zhong, J. Lei, D. X. Yan and Z. M. Li, ACS Appl. Mater. Interfaces, 2019, **11**, 1680-1688.
24. S. Z. Yu, Y. Duan, X. Zhou, Q. L. Xie, G. X. Zeng, X. N. Mao, X. J. Liang, M. Z. Lu, Y. Nie and J. B. Ji, Appl. Therm. Eng., 2019, **153**, 341-351.